A Monte Carlo Event Generator Based on Multi-Chain Model and JACEE High Multiplicity Events

Michio FUKI

Graduate School of Science,
Okayama University of Science, Okayama 700, Japan

(Received September 30, 1986)

ABSTRACT

Three dimensional Monte Carlo event generator available for various kinds of pairs of nucleus-nucleus collisions of the energy greater than tens of GeVs per nucleon is presented. This model is based on the multi-chain model and supplies the inclusive spectra of proton-nucleus and nucleus-nucleus collisions about multiplicity, energy fraction, momentum and rapidity distributions, of leading nucleons and secondary π mesons as well as inelastic cross sections. Then this generator is applied to explain individual nucleus-nucleus collision events observed in cosmic ray experiments with adequate impact parameters. We found that the JACEE high multiplicity events could be explained as small cross sections.

§ 1 INTRODUCTION

Recently the study of high energy nucleus-nucleus collisions of energy greater than 10 GeV per nucleon has become of great interest, not only for nuclear physics but also for particle physics. Because the possibility of a phase transition from nuclear matter to quarkgluon matter, is discussed at the stages of conferences by theoretical physicist's[1] and cosmic ray experimentalists[2] or the view points of close future accelerator experiments[3]. Does such a transition take place[4]? In addition, the BNL energies are in the domain where the effects of baryon and energy stoppings begin to take place[5]. To

investigate those effects at experimental stages, a Monte Carlo event generator for nucleus-nucleus collisions is useful.

In order to describe nucleus-nucleus collisions, we approach from microscopic situation such as a multiple scattering theory. Such models are represented as a nuclear cascading model[6], a wounded nucleon model[7] or a multi-chain model[8]. Particularly the last one has gone well in proton-nucleus collisions as reported on several papers[9]. It is expressed in terms of many integral operators and is so successful as to developing to a Monte Carlo event generator.

The contents in this paper are organized as follows. In § 2 the basic ideas of the model for event generation are explained with assumptions and parametrization methods adopted in this model from inclusive spectra of the experimental proton-proton collision data. The comparison of the prediction from this generator for proton-nucleus collisions with the experimental data is made in § 3. In § 4 several representative nucleus-nucleus collision data of high multiplicity events observed in JACEE experiments are compared with the simulation results. In § 5 discussions and conclusion are given.

§ 2 EVENT GENERATION

Basic ideas of MCM are as follows. Since the nucleus consists of nucleons such as protons and neutrons essentially, the fundamental process of event generation consists in a nucleon-nucleon collision. The Monte Carlo method is adopted to well represent of the experimental data of inclusive distributions of proton-proton collisions. The assumptions and parametrizations for proton-nucleus collisions and nucleus-nucleus collisions in the simulation method are explained.

2 – 1 Assumptions

Basic ideas of collisions for hadron-nucleus and nucleus-nucleus are the following three assumptions.

(1) Nucleon density distribution

The nucleus with mass number A (atomic number Z) consists of A nucleons

(Z protons) as described with nucleon density distribution function[10] based on experiments.

(2) Nucleon leading process

An incoming nucleon or a leading cluster goes on an almost straight line through a target nucleus and collides with nucleons with the same cross section of that of proton-proton collisions even if its energy diminishes in each successive collisions. For incident momentum is enough great with comparing the transverse momentum received by a collision. Thus nucleon-nucleon collisions occur sequentially in a nucleus.

(3) hadron production in a collision

It is assumed that π mesons are produced from a nucleon-nucleon collision but not other unstable mesons and baryons. All π mesons are created outside of the nucleus due to formation zone effect[11]. they will not interact with other nucleons inside of the nucleus and will not interfere one another.

2 – 2 Flow chart of a nucleus-nucleus collision

The essential parameters which decide a nucleus-nucleus collision including a proton-nucleus collision are the types of projectile and target nuclei, mass number A_p , A_t and atomic number Z_p , Z_t , incident energy E_p of a projectile nucleus and impact parameter b_I . The steps of calculation process are explained under these parameters.

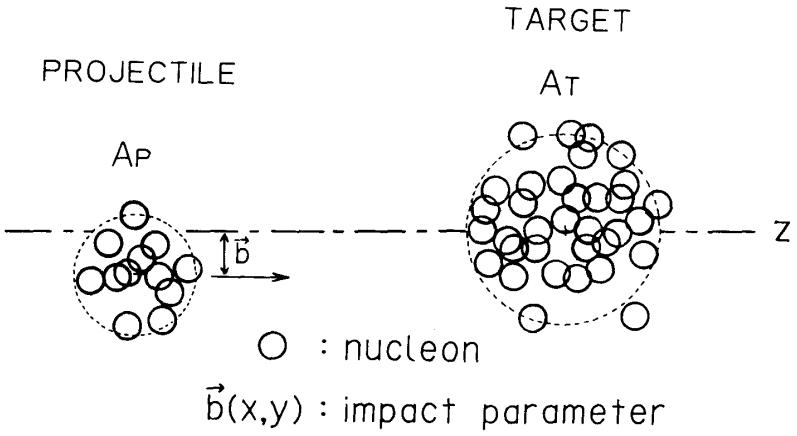

Fig. 1 Schematic View of a nucleus-nucleus collision
A projectile nucleus curbon (A_p=12) collides with a target nucleus iron (A_t=56) by impact parameter b_I. Dotted lines are guide the eye only.

1) To begin with we set the nucleus parameters; (A_p, Z_p), (A_t, Z_t), and the nucleon-nucleon inelastic cross section σ_{NN} dependent on incident energy E_p.

2) The positions of nucleons (x, y, z) inside of projectile and target nuclei are simulated by using nucleon distribution functions. Also the momenta of Fermi motion.

3) Set the impact parameter b_I of projectile and target nuclei.

4) Estimate each impact parameter of the pairs of nucleons between projectile side and target side.

5) Pick up the pairs of nucleons which will collide each other counting collision number N_C.

6) If there are no pairs of collisions, return to the step 3).

7) Ordering the sequence of the pairs of collisions which will take place.

8) Simulate each pair of nucleon-nucleon collision.

9) If the collision number encounters the total collision number N_c, the simulation ends, otherwise go to the step 8).

Schematic view before a nucleus-nucleus collision is shown in Fig. 1. In the 8) step each nucleon-nucleon collision is simulated on the nucleon-nucleon center of mass system and many particles are generated. Then their 4-momenta are transformed to the laboratory system by the Lorentz transformation.

2 – 3 Parametrization of nucleon-nucleon collisions

The schematic view of a nucleon-nucleon collision is shown in Fig. 2. After nucleons interacted each other, the nucleons are scattered and many hadrons are produced.

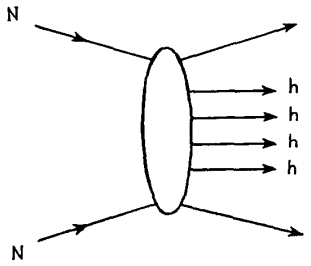

Fig. 2 Conceptual figure of a nucleon-nucleon collision
When nucleons interact each other, a chain is generated and collapses many hadrons.

(1) Leading nucleon spectra

The distribution function of the differential cross section for the leading nucleon is assumed to be independent with the recoil nucleon in the nucleon-nucleon center of mass system. It is parametrized in the longitudinal Lorentz invariant phase space, represented by

$$E\frac{d^3N}{d^3P}=x\frac{2d^3N}{dx\,dP_t^2\,d\phi}=r_N x f(x)g(S,\ P_t)\frac{1}{2\pi} \qquad [1]$$

where

$$x=\frac{E+P_z}{\sqrt{S}}=\frac{M_t}{\sqrt{S}}exp(y) \qquad [2]$$

is the light-like momentum fraction of a leading nucleon and M_t is its transverse mass as defined as $(P_t^2+M^2)^{1/2}$. The rapidity y in center of mass system and $\sqrt{S}$ the total energy of this system. The parameter r_N is the charge non-exchange ratio so the proton to proton ratio is set to 0.6 and the rest is the proton to neutron ratio.

The x distribution function is given as follows. In case of a terminal collision of a leading nucleon and a recoil nucleon,

$$f(x)=1 \qquad [3]$$

This form does not enough include diffractive components. And in case of a successive collision of a leading inside a target nucleus.

$$f(x)=\alpha x^{\alpha-1} \qquad [4]$$

This is referred from ref. (12) ($\alpha = 3$). Low inelasticity of a leading nucleon traveling through a nucleus implies that the energy transfer to a meson cloud is small due to short interaction time. In a terminal collision the energy transfer is given by the same function as the simple proton-proton collision. This sampling is performed on each nucleon-nucleon center of mass system and then the 4-momenta of particles are transformed to the laboratory system by the Lorentz transformation.

The P_t and ϕ are transverse momentum and azimuthal angle, respectively. The P_t distribution function is an exponential one and is expressed by

$$g(S, P_t)=\frac{1}{P_0^2}exp\left(-\frac{P_t}{P_0}\right) \qquad [5]$$

where the parameter P_0 is set to be 0.25 GeV/c. Since the upper limit of the P_t value is restricted by kinematics with the multiplication by a factor of $\sqrt{S}/(\sqrt{S}+P_t)$,

$$P_t \rightarrow P_t\frac{\sqrt{S}}{\sqrt{S}+P_t} \qquad [6]$$

the averaged value $\langle P_t \rangle$ becomes a bit less shan $2P_0$. This leads to the energy dependence of $\langle P_t \rangle$. The x distribution is between $M_t/\sqrt{S}$ and $(E_{max}+P_{zmax})/\sqrt{S}$ by kinematical limitation and is related to the P_t distribution, Energies and z components of momenta are given with equation [2].

$$E=M_t cosh(y), \quad P_z=M_t sinh(y) \qquad [7]$$

As the azimuthal angle ϕ is sampled from a flat distribution from 0 to 2π. The transverse momentum is estimated as follows.

$$P_x=P_t cos(\phi), \quad P_y=P_t sin(\phi) \qquad [8]$$

The similar quantities of the recoil nucleon are generated independently on those of the leading nucleon exçept for the opposite sign of P_z.

(2) Produced hadrons

The inclusive distribution of produced hadrons (actually π mesons) we adopt is given by

$$\frac{2d^3N}{dy\,dp_t^2\,d\phi}=M(E_a)\,h(S, y)\,g(S, p_t)\frac{1}{2\pi} \qquad [9]$$

where $M(E_a)$ is the average multiplicity given by following formula.

$$M(E_a)=1.5[a+b\,ln(E_a/\langle k \rangle)+c\{ln(E_a/\langle k \rangle)\}^2] \qquad [10]$$
$$(a=0.88,\ b=0.44,\ c=0.118)$$

The E_a is available energy for multi-production and $\langle k \rangle$ is mean inelasticity set as 0.5. The parameters a, b and c are taken from the ISR data in ref. (14). The multiplicity distribution is sampled by the KNO-like function such as Gamma distribution (N= 4) for simplicity.

The p_t distribution function $g(S, p_t)$ is the same form as Eq. [5] and [6]. The parameter p_o is set to be 0.18 GeV/c.

And $h(S, y)$ is the rapidity distribution function same as that of Multi-Chain Model ($\nu = 1$) as follows.

$$h(s, y) = G\{(1-x^+)(1-x^-)\}^\beta \qquad [11]$$

where

$$x^\pm = 2m_t exp(\pm y)/\sqrt{S} \qquad [12]$$

The m_t is transverse mass. The parameter β is chosen to be 4 from experimental data of rapidity distribution and G is the normalization factor. The sum of momenta and that of energies of all produced particles must conserve for each nucleon-nucleon collision. A constraint for the conservation of the energy and momentum is introduced in the appendix.

Other weak correlation among particles are not considered and does not seem so significant to our purpose.

(3) Comparison with experimental data of proton-proton collisions

We try to compare the inclusive spectra of proton-proton collisions between this parametrization and experimental data.

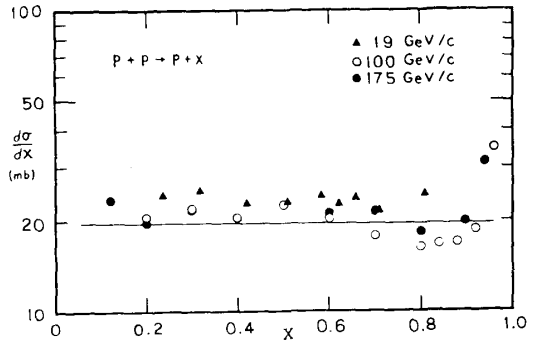

Fig. 3 Proton x distribution
The $x(2E^*/\sqrt{S})$ distribution of protons is roughly constant without diffractive component around $x \sim 1$. The straight line is adopted in simulation.

The inelasticity distribution of protons is represented by the energy fraction $2E^*/\sqrt{S}$ distribution as shown in Fig. 3 are rather consistent in good agreement without diffractive components. The charged multiplicity distribution of secondary particles for typical energy is shown in Fig. 4 . The number of neutral π mesons is sampled from binomial distribution and

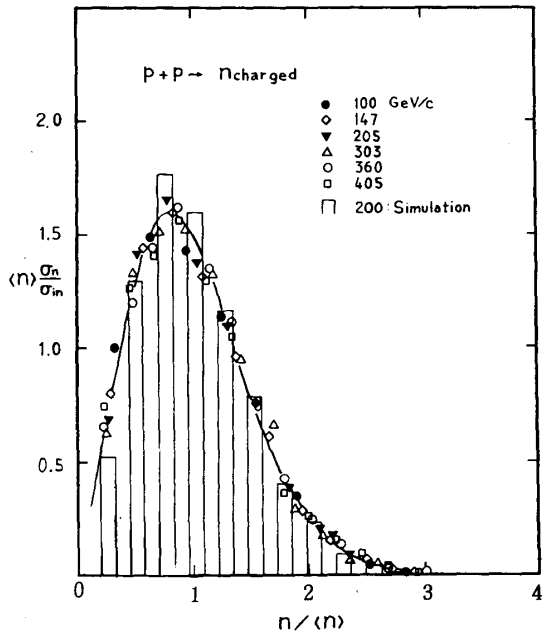

Fig. 4 Example of multiplicity distribution
The points are from experiments[13], a solid line Slattery's[14] empirical formula, histgram from simulation of 2,000 events.

assumed charge symmetry; averaged number is set to $1/3$ of the total π mesons. Even numbers are due to the conservation law of total charge though charge exchange of nucleons. The charged multiplicity distribution thus obtained is compared with the KNO scaling function[14].

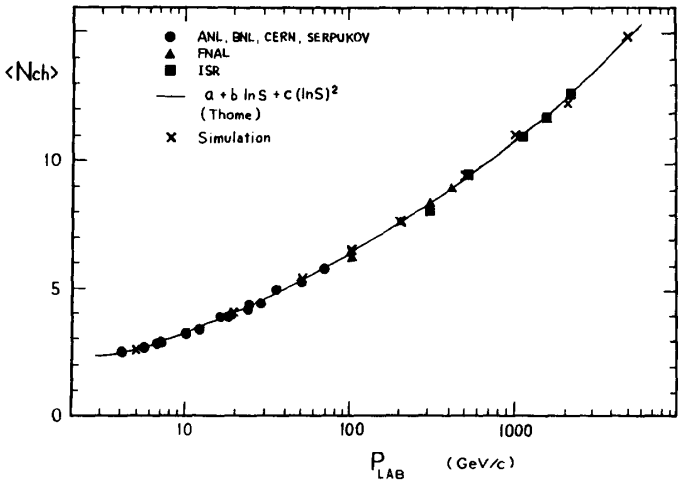

Fig. 5 Energy dependence of average charged multiplicity
A solid line is from Thome et al[15]. × is simulation of 2,000 events.

The energy dependence of averaged multiplicity is shown in Fig. 5 with good agreement of Eq. [10]. The $\langle Nch \rangle / D$ value obtained is close to 2 as shown in Fig. 6 . The average transverse momenta of protons, π mesons and all charged particles are shown in Fig. 7 together with experimental data for comparison. It is shown that the factor of $\sqrt{S}/(\sqrt{S}+P_t)$ leads good agreement with energy dependence of $\langle P_t \rangle$. The Feynman x of protons and pseudo-rapidity distributions of charged pions are also consistent with proton-proton accelerator data around incident energy of 100 GeV.

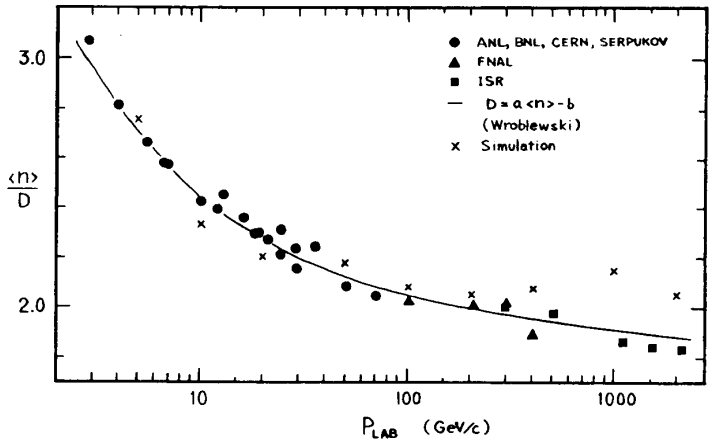

Fig. 6 Energy dependence of $\langle Nch \rangle / D$
Points are from experiments[13]. × is from simulation of 2,000 events.

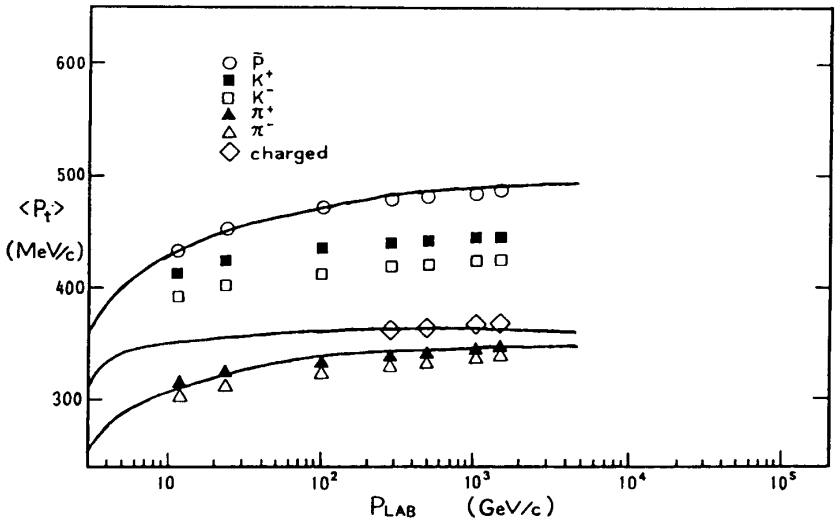

Fig. 7 Energy dependence of average transverse momentum
Points are from experiment[13]. solid lines are from simulation.

Table 1 Proton-nucleus total inelastic cross sections

(unit: mb)

Type :	A_t	Experiments [1]	[2]	[3]	[4]	[5]	[6]	[7]	[8]	Simulation σ_{pA}	ν_{pA}
p + H	1	-	-	-	-	-	32.9	-	33	(33)	(1)
p + D	2	60	-	-	-	-	61.5	-	61	58	1.08
p + He	4	111	-	-	-	-	-	-	102	101	1.30
p + Li	7	-	-	174	208	155	-	-	157	174	1.34
p + Be	9	-	-	210	227	-	-	-	199	215	1.40
p + C	12	269	251	248	254	224	237	-	231	246	1.67
p + O	16	-	-	-	-	-	-	-	292	312	1.69
p + Al	27	-	456	445	472	413	430	438	421	438	2.03
p + Fe	56	-	760	-	-	-	721	-	703	691	2.62
p + Cu	64	-	831	796	850	769	794	856	782	755	2.82
p + Sn	119	-	1255	1259	-	1191	-	1376	1210	1283	3.05
p + W	184	-	-	-	-	-	1691	1943	1650	1724	3.66
p + Pb	207	-	1859	1812	1750	1749	1808	-	1770	1812	3.87
p + U	238	-	2090	2022	-	-	2024	-	1980	2052	3.98

Refs.
[1] Jaros et al.,Phys.Rev.C18(1978)2273: (inelastic, 1.5-2.9 GeV/c)
[2] Bobchenko et al.,Sov.J.Nucl.Phys.30(1979)805: (inelastic, 5-9 GeV/c)
[3] S.P.Denisov et al.,Nucl.Phys.B61(1973)62: (absorption, 6-60 GeV/c)
[4] G.Bellettini et al.,Nucl.Phys.79(1966)609: (absorption, 20 GeV/c)
[5] A.S.Carrol et al.,Phys.Lett.80B(1979)319: (inelastic, 60,200,280 GeV/c)
[6] T.J.Roberts et al.,Nucl.Phys.B197(1979)56: (inelastic, 160-375 GeV/c)
[7] F.Fumuro et al.,Nucl.Phys.B152(1979)376: (absorption, 400 GeV/c)
[8] Rev.Mod.Phys.Vol.56,No.2(1984)S56: (inelastic, 60-375 GeV/c)
(including interpolation of experimental data)

§ 3 PROTON-NUCLEUS COLLISIONS

The generator which was explained in above section, is tested by proton-nucleus collision data in hundreds of GeVs.

3 – 1 Cross sections and collision numbers

Total inelastic cross section of proton-nucleus collisions is estimated as the fractional area of events in which at least one nucleon is hit when many protons run against enough area to include a nucleus with many impact parameters. Table I shows the comparison between simulation results of 100,000 events and some experimental data for various target nuclei. They show good agreement with the experimental data within experimental errors. In this simulation the nucleon-nucleon inelastic cross section was assumed to be 33 mb.

The collision number is counted when the trajectory of a projectile proton comes across a nucleon inside of the target nucleus within a cylinder of the nucleon-nucleon cross-sectional area. The collision number for each event differs from different impact parameters and the variation of target nucleon positions. The averaged collision number $\langle \nu_{pA} \rangle$ has the dependence on mass number A_t of the target nuclei. This dependence can approximately be expressed as follows.

$$\langle \nu_{PA} \rangle = A_t^a, \quad a = 0.23$$

The collision number distribution for target nuclei C (A = 12) and Pb (A = 207) are computed for examples. The result is shown in Fig. 8 together with the estimation of Elias et al[16].

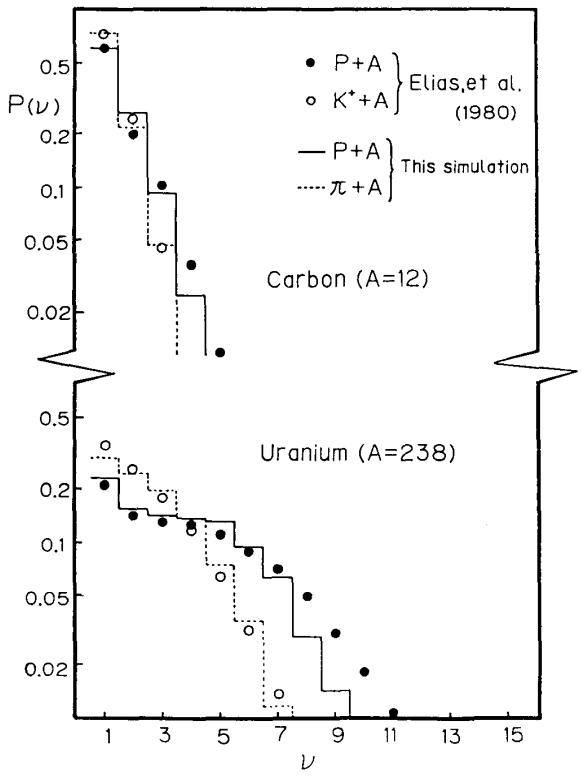

Fig. 8 Examples of collision number distribution in the nucleus
Points are from Elias's[16] analytical calculation, histgrams from simulation of 20,000 events.

3 – 2 Comparison with experimental data

Average charged multiplicities obtained for various target nuclei and incident energy dependence of them are shown in Fig. 9 and the target mass dependence can be written as follows.

$$\langle M \rangle = M_{pp} A_t^b$$

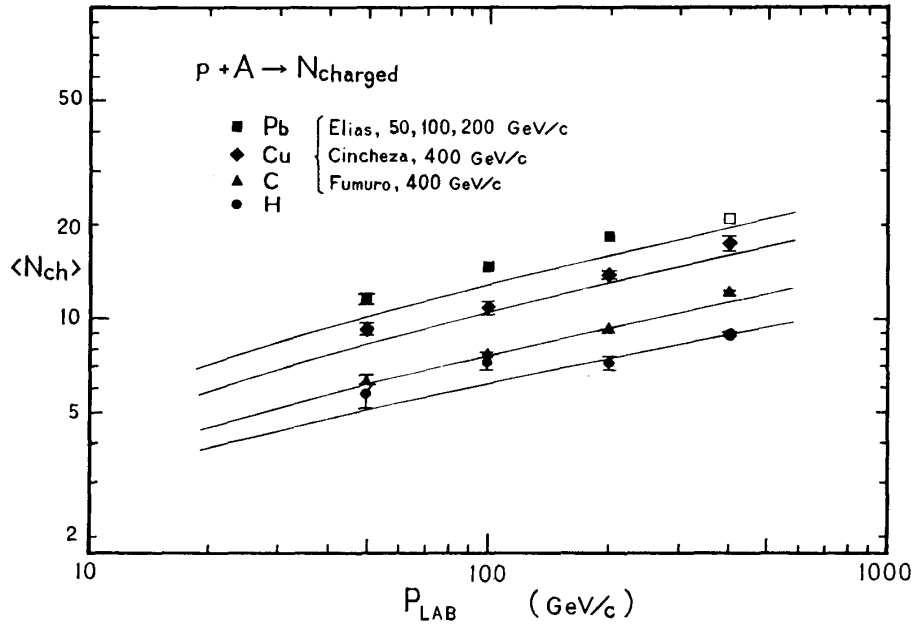

Fig. 9 Energy dependence of averaged multiplicities of proton-nucleus collisions
Points are from experiments[17]. Solid lines are from simulation.

Then M_{pp} is the mean multiplicity of proton-proton collisions. The parameter b has the energy dependence and is about 0.13 around 50 GeV and 0.15 around 400 GeV respectively. In our simulation the multiplicities for carbon target nuclei are seen to be a bit more than the experimental data but on the contrary those for lead target nuclei are seen to be less. However we find that the result for negative particles fits well to the KNO distribution as shown in Fig. 10 and that the $\langle N_{ch} \rangle / D$ value is close to 2.

The inclusive rapidity distribution for various target nuclei are shown in Fig. 11. And the ratio of rapidity densities of negative particles for p-A vs. p-p collisions is compared with experimental data in Fig. 12. They are

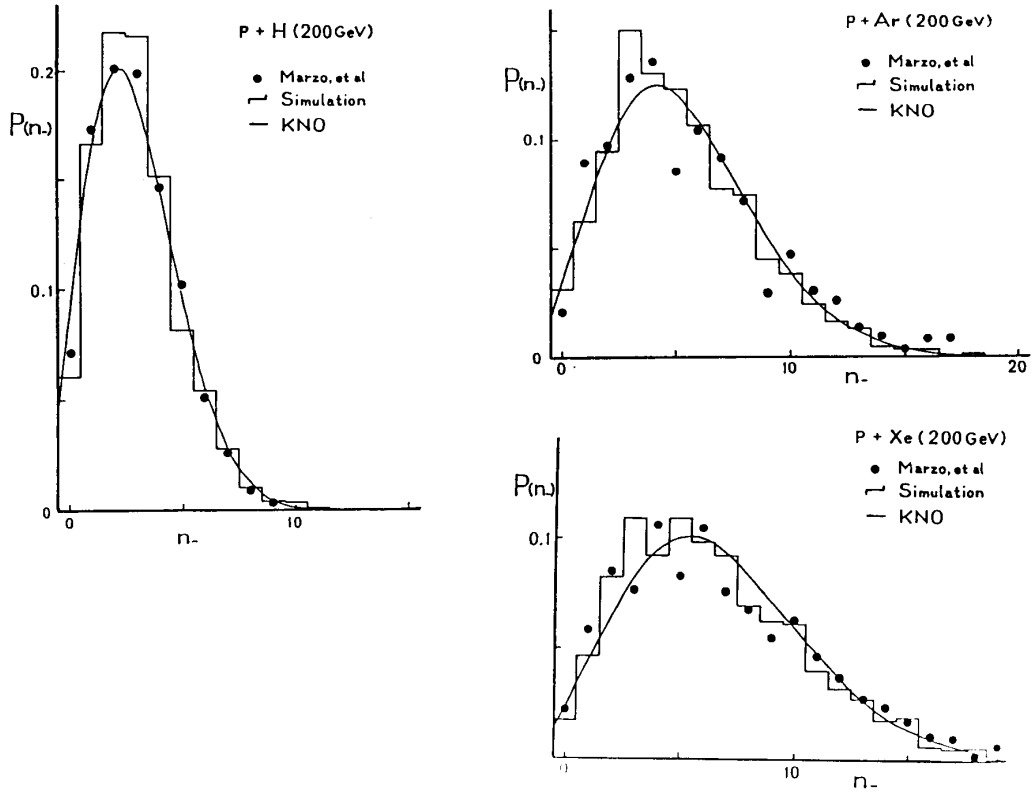

Fig. 10 Examples of negative charged multiplicity distribution
The points are from Marzo's data[18], solid lines Slattery's[14] empirical formula, histgram from simulation of 2,000 events.

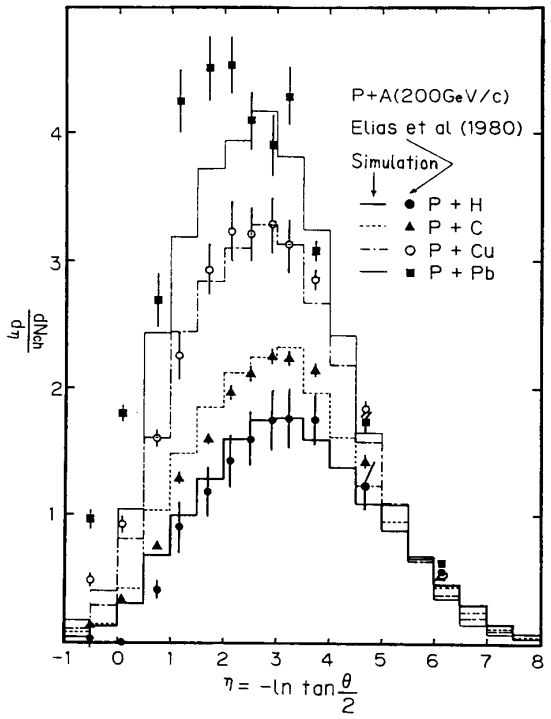

Fig. 11 Pseudo-rapidity distributions for proton-nucleus collisions
The points are from Elias's data[16]. Histgrams are simulation of 2,000 events.

well consistent without the excess of backward region. The decrease less than unity of forward region is explained by absorption of a multi-scattered leading nucleon. In backward region the rapidity density is less than the experimental data for heavy target nuclei. This result may suggest that a part of produced π mesons should interact inside of heavy target nucleus by a cascade process. But this effect will be negligible for light target or in higher energy region as the greater energy has the more multiplicity.

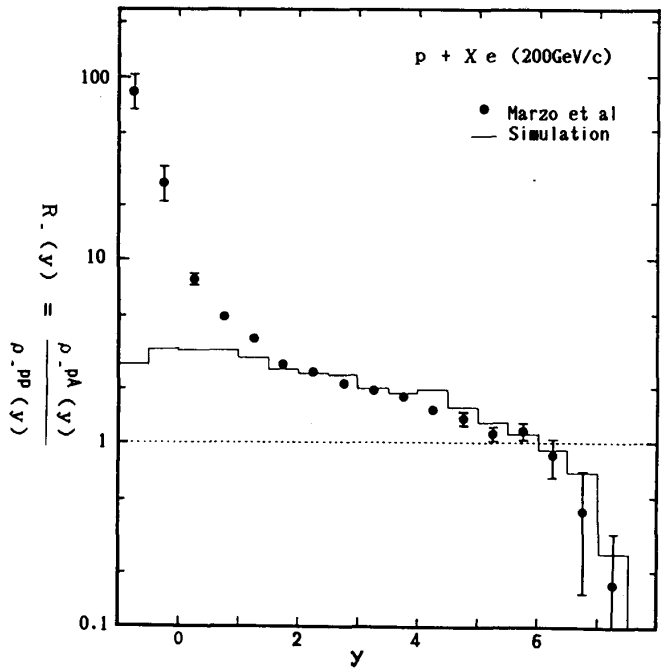

Fig. 12 Example of the ratio of rapidity densities of negative particles Points are from Marzo's[17] and histgram from simulation of 2,000 events.

§ 4 NUCLEUS-NUCLEUS COLLISIONS

4 – 1 Cross sections and collision numbers

Nucleus-nucleus collisions are simulated for events of 100,000 impact parameters and the total inelastic cross sections are estimated by the same manner as in the case of proton-nucleus collisions. In the simulation, the collision order is determined by the incident distances between each nucleon of the projectile side and that of the target side. We call collided nucleons as wounded nucleons.

Table 2 Nucleus-nucleus total inelastic cross sections

(unit: mb)

Type A + B	Experiments (1)	(2)	(3)	(4)	Empiricals (5)	(6)	Simulation (σ_{NN}=33mb) σ_{AB}	N_A	N_B	N_C
^{2}D + ^{2}D	-	134	-	-	103	114	97	1.2	1.2	1.3
^{2}D + ^{4}He	-	204	-	-	184	166	166	1.2	1.4	1.6
^{2}D + ^{12}C	-	426	-	-	401	322	356	1.4	2.1	2.3
^{4}He + ^{4}He	-	276	-	262	289	257	251	1.7	6.0	6.5
^{4}He + ^{9}Be	-	-	-	485	467	384	452	1.7	1.7	2.1
^{4}He + ^{12}C	-	535	-	503	550	446	479	1.9	2.0	2.6
^{4}He + ^{27}Al	-	-	-	780	868	689	756	2.0	2.6	3.3
^{4}He + ^{56}Fe	-	-	-	-	1310	1040	1102	2.3	3.6	4.6
^{4}He + ^{207}Pb	-	-	-	-	2780	2250	2252	2.5	5.2	6.6
^{12}C + ^{12}C	826	888	-	-	895	820	818	2.9	8.9	11.5
^{12}C + ^{16}O	1022	-	-	-	1020	918	954	3.6	3.6	5.8
^{12}C + ^{56}Fe	-	-	1660	1610*	1820	1580	1581	3.9	4.1	6.6
^{12}C + ^{64}Cu	1730	-	-	-	1940	1680	1679	5.3	8.6	13.9
^{12}C + ^{207}Pb	2960	-	-	-	3490	3020	3259	5.4	9.2	14.8
^{16}O + ^{56}Fe	-	-	-	-	1990	1788	1831	7.0	16.7	27.0
^{16}O + ^{64}Cu	1950	-	-	-	2120	1896	1899	6.2	9.8	16.3
^{16}O + ^{207}Pb	3270	-	-	-	3730	3294	3462	6.4	10.5	17.8
^{6}Fe + ^{64}Cu	-	-	2940	-	3220	3156	2832	15.3	16.0	42.2
^{56}Fe + ^{207}Pb	-	-	5100	-	5150	4900	4791	21.4	30.5	79.2

Refs.
(1) Lindstorm et al.,Bull.Am.Phys.Soc.17(1972)488
(2) Jaros et al.,Phys.Rev.C18(1978)2273
(3) Westfall et al.,Phys.Rev.C19(1979)1309: (mass changing, 1.88GeV/n)
(4) Tanihata et al.,Phys.Lett.160B(1985)380
* Webber et al.,Ap.J.260(1982)894 ,(mass changing, 0.98GeV/n)
(5) Heckman et al.,Phys.Rev.C17(1978)1735: (total reaction, 2.1GeV/n)
(6) Hagen et al.,Ap.J.212(1977)262: (total inelastic)

Table 2 shows the comparison of inelastic cross section among the simulation results, empirical formula and experimental data. They agree well each other within the experimental errors of 4 %. Here the inelastic cross section for nucleon-nucleon collisions is set to 33 mb.

Wounded nucleon number distributions of projectile nuclei, those of target nuclei and collision number distributions can be calculated for any fixed impact parameters.

4 − 2 Multiplicity frequency

Table 3 shows the differences between representative cosmic ray high

Table 3 High multiplicity events

Type	Observed E_0(TeV/n)	N_{obs}	$dN_{obs}/d\eta$	Simulation (b=0) N_{ch}^*	$dN_{ch}/d\eta$	Frequency $P(>N_{obs})$	$\sigma(>N_{obs})$
Ca + Pb ···(1)	1.5	1050 +300,-50	258	1350 ± 79	305 ± 18	0.062	280 (mb)
Si + Ag ···(2)	4.0	1010 ± 30	184	1074 ± 85	215 ± 16	0.029	90
Ca + C	100.	760 ± 30	81	830 ± 97	114 ± 12	0.022	37
Li + C	15.	217 ± 15	37.5 ± 4.3	165 ± 45	28 ± 6.3	0.017	13
He + C	20.	148 ± 10	26.5 ± 3.6	133 ± 34	18 ± 4.4	0.049	27
Ti + Pb ···(3)	0.041	267	125	438 ± 27	155 ± 12	-	-
Ti + Ag	0.026	265	95	287 ± 17	104 ± 11	0.017	60
Fe + C	0.05	128	40	117 ± 13	32 ± 5.7	0.010	16

N_{obs}, N_{ch} : multiplicity observed and average charged multiplicity simulated
dN_{ch}/dy : rapidity density at $y^*= 0, \pm\delta$ for $\Delta y^* < 1$

Refs.
(1) T.H.Burnett et al, Proc.19th ICRC(La Jolla),2(1985)76,HE1.4-4
(2) T.H.Burnett et al, Phys.Rev.Lett.,50,20(1983)2062
(3) T.H.Burnett et al, Proc.19th ICRC(La Jolla),2(1985)72,HE1.4-3

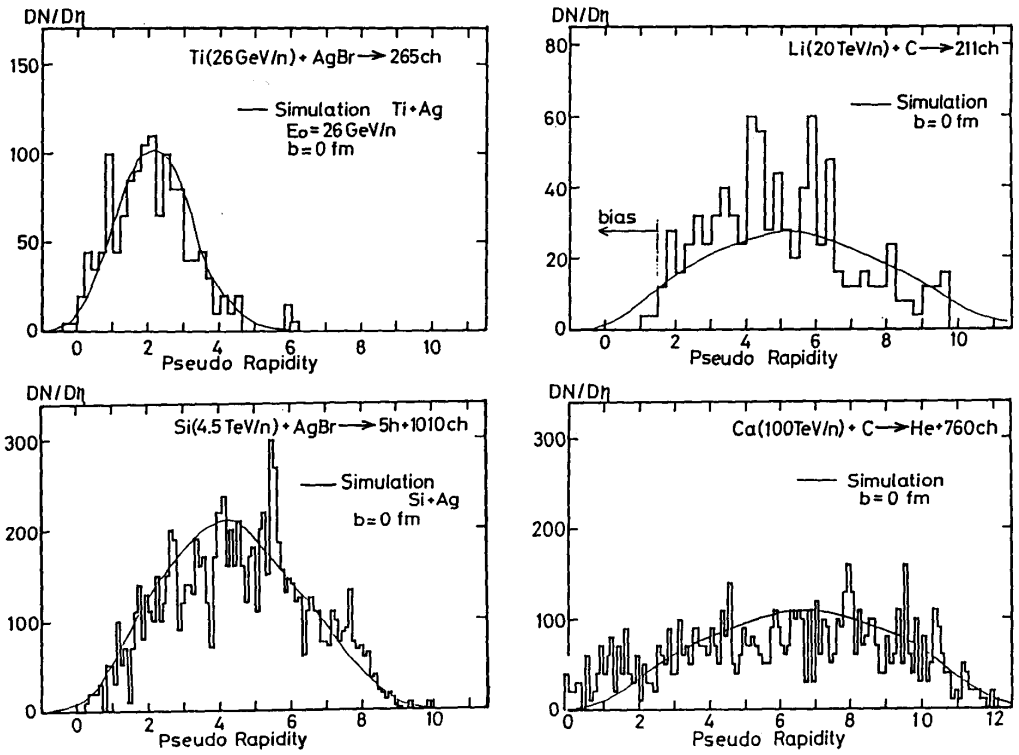

Fig.13 Comparison of pseudo-rapidity distributions with cosmic-ray high multiplicity events
Simulation data are averaged by 200 events with condition of $b_I = 0$.
Histgrams are from JACEE[18].

multiplicity events from the JACEE[18]experiment and the simulation results obtained by choosing suitable impact parameters. In these calculations the energy dependence of nucleon-nucleon inelastic cross section is considered.

Fig. 13 shows the pseudo-rapidity distribution of representative cosmic ray events. The simulation results can be made to agree with experimental data. But for a fraction of events, the multiplicity is a little less than experimental data even if by taking $b_I = 0$. Next the multiplicity distributions by taking b_I free is shown in Fig. 14 respectively. And the frequencies that exceed the observed multiplicities are listd in Table 3 . They are small cross sections.

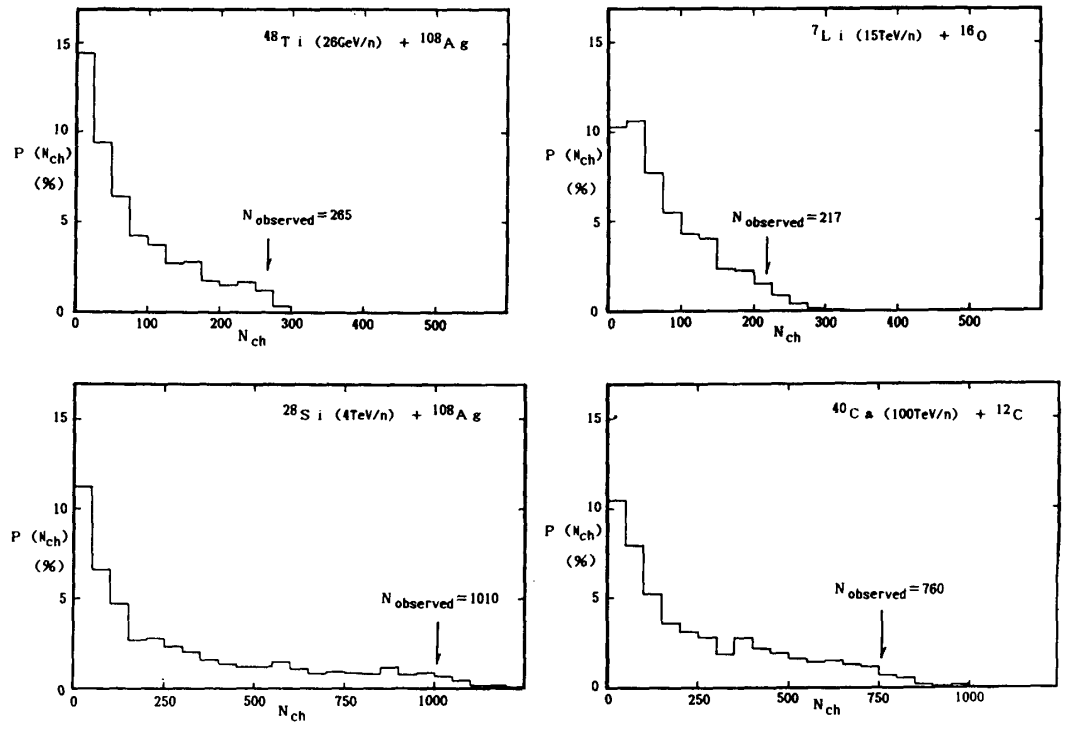

Fig. 14 Charged multiplicity distributions of nucleus-nucleus collisions Simulation was done for all impact parameters with same energies of cosmic ray events.

§ 5 DISCUSSIONS AND CONCLUSION

A Monte Carlo event generator for a nucleus-nucleus collision constructed on the basis of MCM and the traditional hypotheses is rather successful for explanation of accelerator proton-nucleus inclusive data and cosmic ray nucleus-nucleus individual events. But in details the results do not fit within a 10% error to proton vs. heavy nucleus collision. This seems to be due to an unknown process which may be due to cascading of produced particles. In the future, for the more close agreement between simulation results and experimental data, it will be necessary to include that effect. Moreover for necessity, Kaons, unstable mesons, hyperons, a diffractive Pomeron process, large P_t components, some particle correlation and so on.

The high multiplicity events from JACEE experiment can be represented by this generator due to cross sections less than 5 %. Therefore the JACEE experiment has some events of very rare frequencies. And the high $\langle P_t \rangle$ phenomena seem to be difficult to represent by this event gererator. More detail discussion in consideration of cosmic ray flux is needed.

Appendix —— Compulsive energy-momentum conservation

Total energy and momentum of all secondary particles are constrained to conserve before and after interaction. In order to impose this principle on N particles, the following equations for constraint are given.

$$\sum_i^N \{f(P_{iw}-a_w)\}=\triangle P_w \ , \quad (w=x,\ y)$$

$$\sum_i^N \{f(P_{iz}-E_i a_z)\}=\triangle P_z \ ,$$

$$\sum_i^N [m_i^2+\{f(P_i-E_i a)\}^2]^{1/2}=\triangle E$$

where $\triangle P(\triangle P_x,\ \triangle P_y\ ,\ \triangle P_z)$ and $\triangle$ E are the sums of momenta and energies excluding leading particles. Then E_i and m_i are the energy and mass of each particle. The parameters f and $a(a_x,\ a_y\ ,\ a_z)$ are solved by the iteration method. Thus the sets of new momenta are substituted as follows.

$$P_{iw} \rightarrow f(P_{iw}-a_w) \qquad (w=x,\ y)$$

$$P_{iz} \rightarrow f(P_{iz}-E_i a_z)$$

$(i = 1, 2, \cdots\cdots, N)$

If the f falls outside of the range from 0.5 to 2.0, these sets are excluded and another new sets are sampled. The distortion of momentum distribution obtained by this method seems to be small.

ACKNOLEDGEMENT

I thank very much to Prof. K. Imaeda about his interest and advice to this theme. Also thank to Dr. H. Sumiyoshi about his earnest discussions. I am in debt of JACEE members about useful advice and discussions for experiments.

The computer simulation was carried out with FACOM-M380S in computer center in Okayama University of Science and FACOM-M 380 in Institute for Nuclear Study in University of Tokyo. The funds owe to these institutes.

References

1) Proceedings of International Conference on Ultra-Relativistic Nucleus-Nucleus Collisions, "Quark Matter '82, '83, '84, '85", For examples, Nucl. Phys. *A 418* (1984), Nucl. Phys. *A 447* (1986)
2) Proceedings of International Cosmic Ray Conference, For examples, Proc. 19th ICRC (La Jolla) (1985) HE. Sec.
3) S. Nagamiya, Hyperfine Interactions 21, 219
4) J. D. Bjorken, Phys. Rev., *D27* (1983) 140
5) S. Date, M. Gyulassy, H. Sumiyoshi, Phys. Rev., *D32*, 3 (1985) 619
6) J. Cugnon, Phys. Rev., *C22*, 5 (1980) 1885
Y. Kitazoe, et al., Phys Lett., *138B*, 5, 6 (1984) 341
Y. Kitazoe, et al., Phys Rev., *C29*, 3 (1984) 828
7) A. Bialas, M. Bleszynski, W. Czyz, Nucl. Phys., *B111* (1976) 461
F. Takagi, Prog. Theor. Phys., *64*, 4 (1980) 1334
8) K. Kinoshita, A. Minaka, H. Sumiyoshi, Z. Phys., *C8* (1981) 205
9) K. Kinoshita, A. Minaka, H. Sumiyoshi, Prog. Theor. Phys., *61* (1979) 165
C. Wong, Phys. Rev., *D30*, 5 (1984) 972, Phys. Rev. Lett., *52*, 16 (1984) 1393
10) N. N. Nikolaev, Sov. J. Part., 12 (1981) 63
11) K. Kinoshita et al., Prog. Theor. Phys., *63*, 3 (1980) 94
12) R. J. Glauber and G. Matthiae, Nucl. Phys., *B21* (1970) 135
13) G. Giacomelli and M. Jacob, Physics Reports *55*, 1 (1979) 1
14) P. Slattery, Phys. Rev., *D7*, 7 (1973) 2073

15) W. Thome et al., Nucl. Phys., *B 129* (1977) 365
16) J. E. Elias et al., Phys. Rev., *D22*, 1 (1980) 13
17) C. De Marzo et al., Phys. Rev., *D26*, 5 (1982) 1019
18) T. H. Burnett et al., Phys. Rev. Lett., *50*, 20 (1983) 2062
T. H. Burnett et al., Proc. 19th ICRC (La Jolla), *2* (1985) 72, 76